Highly Efficient Polymer Light-Emitting Diodes Using Graphene Oxide as a Hole Transport Layer

Bo Ram Lee,[†,‡] Jung-woo Kim,[‡,§] Dongwoo Kang,[‡,§] Dong Wook Lee,[⊥] Seo-Jin Ko,[§] Hyun Jung Lee,[†] Chang-Lyoul Lee,[∥] Jin Young Kim,[§] Hyeon Suk Shin,[‡,§,*] and Myoung Hoon Song[†,‡,*]

[†]School of Mechanical and Advanced Materials Engineering, [‡]Low Dimensional Carbon Materials Center, and [§]Interdisciplinary School of Green Energy, and KIER-UNIST Advanced Center for Energy, Ulsan National Institute of Science and Technology (UNIST), UNIST-gil 50, Ulsan 689-805, Republic of Korea, [⊥]LG Electronics, Advanced Research Institute 38, Baumoe-ro, Seocho-gu, Seoul 137-724, Republic of Korea, and [∥]Advanced Photonics Research Institute, Gwangju Institute of Science and Technology, 1 Oryong-dong Buk-gu, Gwangju 500-712, Republic of Korea

ABSTRACT We present an investigation of polymer light-emitting diodes (PLEDs) with a solution-processable graphene oxide (GO) interlayer. The GO layer with a wide band gap blocks electron transport from an emissive polymer to an ITO anode while reducing the exciton quenching between the GO and the active layer in place of poly(styrenesulfonate)-doped poly(3,4-ethylenedioxythiophene) (PEDOT:PSS). This GO interlayer maximizes hole–electron recombinations within the emissive layer, finally enhancing device performance and efficiency levels in PLEDs. It was found that the thickness of the GO layer is an important factor in device performance. PLEDs with a 4.3 nm thick GO interlayer are superior to both those with PEDOT:PSS layers as well as those with rGO, showing maximum luminance of 39 000 Cd/m^2, maximum luminous efficiencies of 19.1 Cd/A (at 6.8 V), and maximum power efficiency as high as 11.0 lm/W (at 4.4 V). This indicates that PLEDs with a GO layer show a 220% increase in their luminous efficiency and 280% increase in their power conversion efficiency compared to PLEDs with PEDOT:PSS.

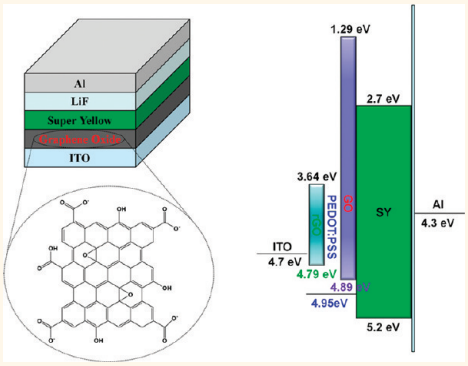

KEYWORDS: graphene oxide · polymer light-emitting diodes · hole transport layer · super yellow

Polymer-based optoelectronics have been researched over the past few decades. In particular, polymeric light-emitting diodes (PLEDs) have been investigated for displays, solid-state lightening, and flexible electronic devices.[1−7] For commercial application, extensive research efforts have been devoted to improving the efficiency and stability of PLEDs. Nevertheless, considerable room for improvement with regard to the efficiency and stability of PLEDs remains.

Charge injection/transport layers are very important components in high-performance optoelectronics such as PLEDs and organic photovoltaics (OPVs).[8−10] Particularly, the interfaces between the charge transport layer and the emissive semiconducting layer are crucial in the operating characteristics, the stability, and the performance of the devices.[11−13] Poly(styrenesulfonate)-doped poly(3,4-ethylenedioxythiophene) (PEDOT:PSS) is usually used as the hole transport layer (HTL) as it reduces the contact barrier between the ITO and the active semiconducting polymers and reduces the ITO roughness upon coating with it. However, a highly acidic aqueous solution of PEDOT:PSS can gradually corrode an ITO electrode[14] and eventually degrade the performance and long-term stability of devices.[15] Moreover, significant quenching of radiative excitons normally occurs between PEDOT:PSS and an emissive semiconductor interface,[16] despite the fact that PEPOT:PSS is a good HTL with high electric conductivity. Recently, many groups have tried to replace PEDOT:PSS layers or use a thin buffer layer between PEDOT:PSS and the emissive layer interface to reduce exciton quenching.[17−21] Moreover, thin metal oxide films of MoO_3,[22−29] WO_3,[30,31] NiO,[32,33] V_2O_5,[28,34,35] and Fe_3O_4[36] were suggested for the efficient charge transport of organic optoelectronics with excellent air-stability, optical transparency, and mechanical robustness.[24−27,30] However, the requirement of a vacuum evaporation technique for semiconducting metal oxides makes the fabrication process complex. Therefore, the motivation behind our research is to find a suitable solution-processable substitute for PEDOT:PSS to overcome the current limitations

* Address correspondence to mhsong@unist.ac.kr, shin@unist.ac.kr.

Received for review November 9, 2011 and accepted March 5, 2012.

Published online March 05, 2012
10.1021/nn300280q

with regard to device performance/efficiency and stability.

Chemical vapor deposition (CVD)-grown graphene[4,37−39] and reduced graphene oxide (rGO)[40−45] have been studied as promising alternatives for ITO for transparent electrodes in organic optoelectronic devices due to the optical transparency, mechanical flexibility, and high electroconductivity of these materials.[46−53] Recently, GO as a HTL was introduced in organic solar cells (OSCs).[54,55] The efficiency of OSCs with a GO layer was comparable to devices fabricated with PEDOT:PSS. On the other hand, GO functionalized with 4-octoxyphenyl diazonium tetrafluoroborate was utilized as a HTL in organic LEDs (OLEDs), showing that the efficiency of OLEDs with a functionalized GO layer was enhanced by 150% compared to the reference device with PEDOT:PSS.[56] However, there is a lack of supporting data regarding the origin of the improved efficiency, such as data pertaining to the energy alignment and characterization of the functionalized GO.

Here we demonstrate a direct method to improve the efficiency and performance of PLEDs with solution-processable graphene oxide (GO) as a HTL. This GO interlayer of an optimum thickness prevents significant quenching of the radiative excitons between the emissive polymer and the GO layer and enables balanced electron and hole injection by blocking the electrons from SY to the ITO, thus enhancing both device performance and efficiency in PLEDs. Furthermore, the mechanism of enhanced performance by a GO layer is supported by the electron-blocking behaviors of the GO layers and by a comparison of the photoluminescence (PL) intensities and V_{oc} measurements in organic photovoltaic devices.

RESULTS AND DISCUSSION

Figure 1a presents the complete device architecture of PLEDs using negatively charged GO. The PLEDs were prepared by the sequential deposition of ITO (150 nm) as a transparent anode, GO as a HTL, poly(phenylvinylene): super yellow (SY, Merck Co., M_w = 1 950 000 g mol^{-1}) (150 nm) as an emissive layer, LiF (1 nm) as an electron injection/transporting layer (EIL/ETL), and Al (70 nm) as metallic cathode. The chemical structure of negatively charged GO contains chemical functional groups such as carboxyl, hydroxyl, and epoxy groups. The functional groups, in this case the epoxy and hydroxyl groups, disrupt the sp^2 conjugation of the hexagonal graphene lattice in the basal plane. Thus, GO behaves as an insulator with a large band gap of around 3.6 eV.[54] The Fermi level of the GO used in this study was about 4.89 eV, whereas the Fermi level of the rGO used in this study was about 4.79 eV according to ultraviolet photoemission spectroscopy (UPS) measurements (see Figure 4a,b below). The reduction of GO removes the functional groups in the GO

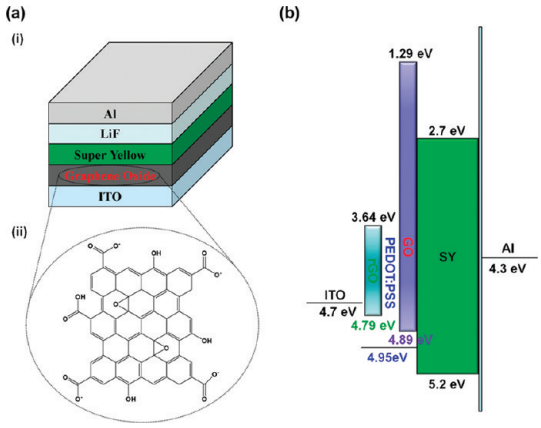

Figure 1. (a) Device schematics of PLEDs with a GO layer and the chemical structure of the GO. (b) Schematic energy diagrams of the flat band conditions of PLEDs with a HTL (rGO, GO, and PEDOT:PSS).

sheets, partially restores sp^2 conjugation, and therefore reduces the band gap to 1.15 eV.[57] The rGO with the decreased band gap shows different behavior from a GO layer in the PLEDs (see Figure 3 and Table 1 below).

Figure 2 shows atomic force microscopy (AFM) images of four GO films on substrates. The morphology and thickness of the GO films depend on the number of spin-coated layers. It was difficult to fabricate full-coverage GO films by spin-coating on ITO substrates only once or twice (Figure 2a,b). However, Figure 2b shows connected GO sheets despite the vacant sites that exist. Additional repetitions of spin-coating led to the desired full coverage of GO films, and the average thicknesses of the GO films in Figure 2c,d were measured to be approximately 4.3 and 5.3 nm, respectively, by ellipsometry.

The device characterizations of PLEDs with/without PEDOT:PSS, with rGO, and with different thickness of the GO layer are presented in terms of (a) the current density *versus* the applied voltage ($J-V$), (b) the luminance *versus* the applied voltage ($L-V$), (c) the luminous efficiency *versus* the voltage ($E-V$), and (d) the power efficiency *versus* the voltage ($P-V$), as shown in Figure 3. We note that all of the devices represented the original green emission of SY regardless of the type of HTL or the applied voltages, as shown in Figure S1 in the Supporting Information. Reference PLEDs with PEDOT:PSS showed a maximum luminance of 33 800 cd/m^2 (at 12.6 V) and luminous efficiency of 8.7 cd/A (at 9.6 V). For PLEDs with a rGO layer, the maximum luminance (8300 cd/m^2 at 13.0 V) and luminous efficiency (5.0 cd/A at 8.6 V) were much lower than those of PLEDs with PEDOT:PSS due to the lower conductivity of the rGO layer and the lower hole injection caused by the higher contact barrier between the rGO and the SY. In contrast, PLEDs with a GO layer showed enhanced EL efficiency and luminance. Among different conditions of GO layers, optimized PLEDs using a 4.3 nm thick GO film with full coverage exhibited the highest luminance value of 39 000 cd/m^2 (at 10.8 V), highest luminous

TABLE 1. Device Performances of PLEDs with Different Hole Transport Layers

device configuration	maximum luminance (cd/m^2) (at voltage)	maximum luminous efficiency (cd/A) (at voltage)	maximum power efficiency (lm/W) (at voltage)	maximum EQE (%) (at voltage)	turn on voltage (V)
ITO/SY/LiF/Al	700 (16.0 V)	1.4 (8.4 V)	0.6 (6.6 V)	0.6 (8.4 V)	2.8
ITO/PEDOT:PSS/SY/LiF/Al	33800 (12.6 V)	8.7 (9.6 V)	3.9 (5.2 V)	3.5 (9.2 V)	1.8
ITO/GO[2.0 nm]/SY/LiF/Al	31400 (12.4 V)	8.8 (9.4 V)	4.2 (5.0 V)	3.3 (8.2 V)	1.8
ITO/GO[2.6 nm]/SY/LiF/Al	35100 (12.0 V)	14.3 (8.6 V)	6.6 (5.4 V)	5.0 (8.4 V)	1.8
ITO/GO[4.3 nm]/SY/LiF/Al	39000 (10.8 V)	19.1 (6.8 V)	11.0 (4.4 V)	6.7 (6.8 V)	1.8
ITO/GO[5.2 nm]/SY/LiF/Al	28500 (11.2 V)	13.9 (7.4 V)	8.6 (4.0 V)	5.0 (7.4 V)	1.8
ITO/rGO[4.3 nm]/SY/LiF/Al	8300 (13.0 V)	5.0 (8.6 V)	2.0 (6.2 V)	1.8 (8.6 V)	1.8

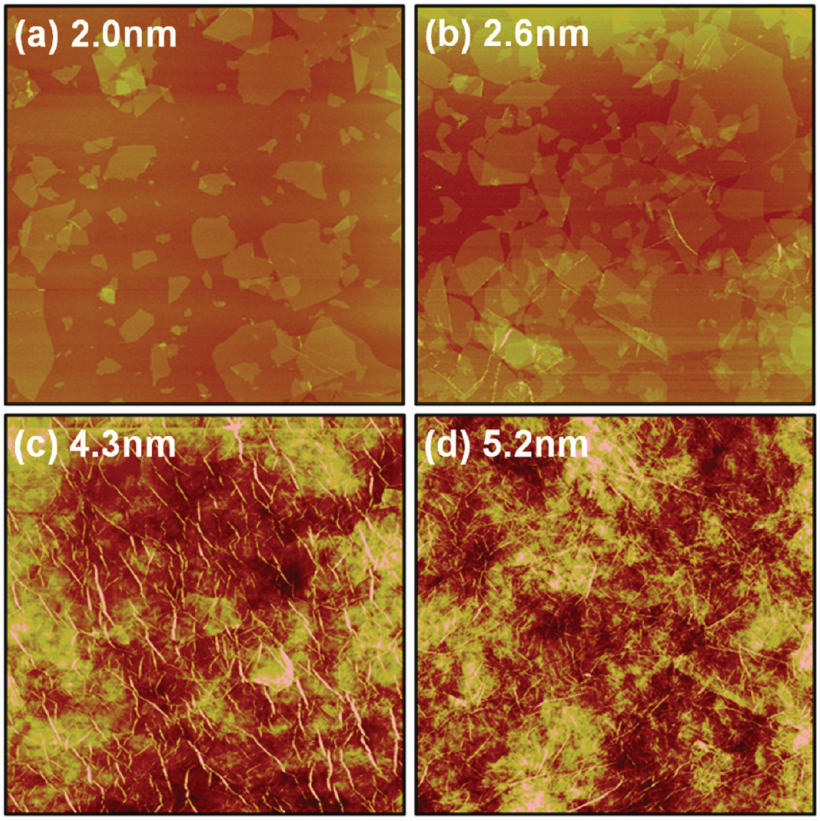

Figure 2. AFM images of different thicknesses of GO of approximately (a) 2.0 nm, (b) 2.6 nm, (c) 4.3 nm, and (d) 5.3 nm.

efficiency value of 19.1 cd/A (at 6.8 V) and highest power efficiency value of 11.0 lm/W (at 4.4 V), which were enhanced by roughly 120, 220, and 280%, respectively, compared to the conventionally structured devices with PEDOT:PSS. From the energy level diagram shown in Figure 1b, the electron blocking of the GO film with a large band gap from the SY to the ITO anode can be expected, which was different from the rGO film with a small band gap. This electron-blocking effect optimized the electron−hole recombination probability within the emissive SY layer and therefore enhanced the device performance and efficiency in PLEDs. Here, we emphasize that it is quite important to find the optimum thickness of the GO layer for high performance and feasible efficiency of PLEDs. The thinner GO films did not bring the best results due to their poor electron-blocking behavior, whereas the thicker GO film degraded the device performance and efficiency due to the increase in the contact resistance, resulting in lower hole injection/transfer. Note that the efficiency of the PLED with the thin GO layer in Figure 3b is still better than that with PEDOT:PSS, which is consistent with the result by Zhong *et al.*[56] The detailed device characteristics are summarized in Table 1. The performance and efficiency of OLEDs with a GO layer as a HTL will be still enhanced even though phosphorescent materials are used instead of SY as active materials. We plan to use the phosphorescent-based iridium complexes in future study. As for the lifetime of devices, Yun *et al.* has already demonstrated that the lifetime of the rGO-based organic solar cell is better than that of the

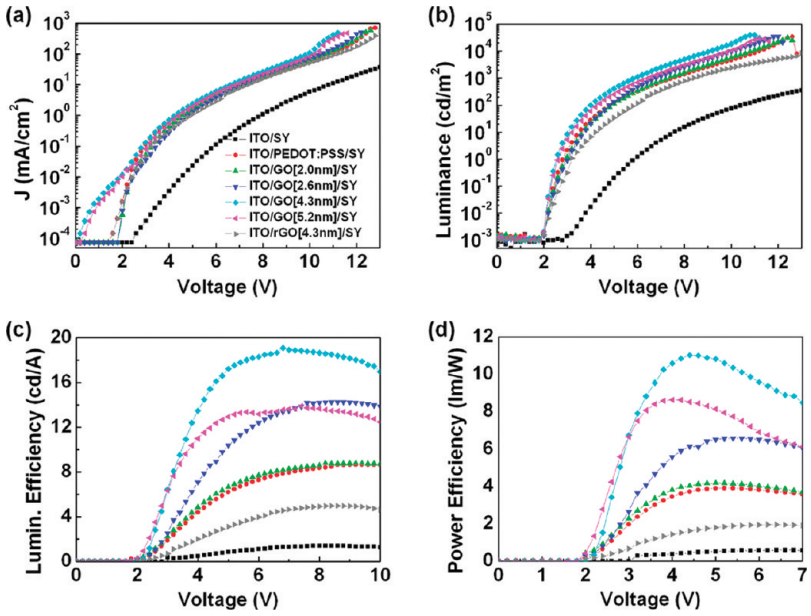

Figure 3. (a) Current density *vs* applied voltage (*J*−*V*), (b) luminance *vs* the applied voltage (*L*−*V*), (c) luminous efficiency *vs* the applied voltage (*E*−*V*), and (d) power efficiency *vs* the applied voltage (*P*−*V*) curves for various charge transport layers.

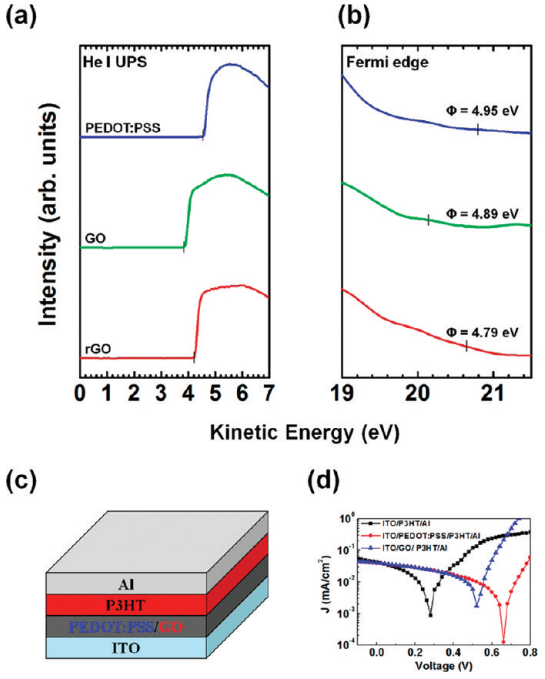

Figure 4. Ultraviolet photoemission spectroscopy (UPS) spectra of rGO, GO, and PEDOT:PSS HTLs: (a) inelastic cutoff region and (b) Fermi edge region. (c) Device structure of OPVs and (d) *J*−*V* characterization of OPVs with/without a hole transport layer (HTL) (PEDOT:PSS or GO).

PEDOT:PSS-based organic solar cell due to the highly acidic (pH ~ 1) suspension of PEDOT:PSS.[55] Therefore, the lifetime of the GO-based PLED is also expected to be better than the PEDOT:PSS-based one.

To confirm the energy levels of GO, rGO, and PEDOT:PSS, ultraviolet photoelectron spectroscopy (UPS) measurements were performed. From the UPS measurements, the work function values were calculated from the difference between the inelastic cutoff and the Fermi edge, as shown Figure 4a,b. While the PEDOT:PSS layer showed a work function of 4.95 eV, GO and rGO showed values of 4.89 and 4.79 eV, respectively. Photovoltaic measurements were also conducted to confirm the work function values by the UPS measurements. The device structure of OPVs, as prepared by the sequential deposition of ITO, PEDOT:PSS, or GO, poly(3-hexylthiophene) (P3HT, Merck Co., M_w = 75 000 g mol^{-1}, RR > 97%), and Al, is presented in Figure 4c. The *J*−*V* curves of these devices were measured under AM 1.5G illumination at 100 mW/cm^2. Generally, the V_{oc} value of a metal−insulator−metal (MIM) device is determined by the difference in the work function values of the two metal contacts.[58] In the OPV structures here, the different values of V_{oc} were influenced by the different work function of the PEDOT:PSS and the GO-modified ITO, while the work function of the Al cathode was fixed. The V_{oc} value of the OPVs with the GO layer was lower (0.53 V) than that with PEDOT:PSS (0.66 V), as shown in Figure 4d. As a result, we confirmed the work function of GO and PEDOT:PSS, as shown in Figure 1b.

Figure 5a,b shows the architecture of the PLEDs and the electroluminescence (EL) spectra of the devices to demonstrate the electron-blocking behavior of the GO layers used in this work. The devices include two light-emitting polymer layers of SPR-001 (red-light-emitting polymer, Merck Co.) and SY (green-light-emitting polymer, Merck Co.). The structure of SPR-001 is unknown. It was difficult to deposit the hydrophilic GO film successfully by spin-casting it onto the hydrophobic SPR-001 or SY in a polymer/GO/polymer device structure. To coat a GO film, we performed a brief UV/O_3 treatment for 30 s on the polymer surface, after which we

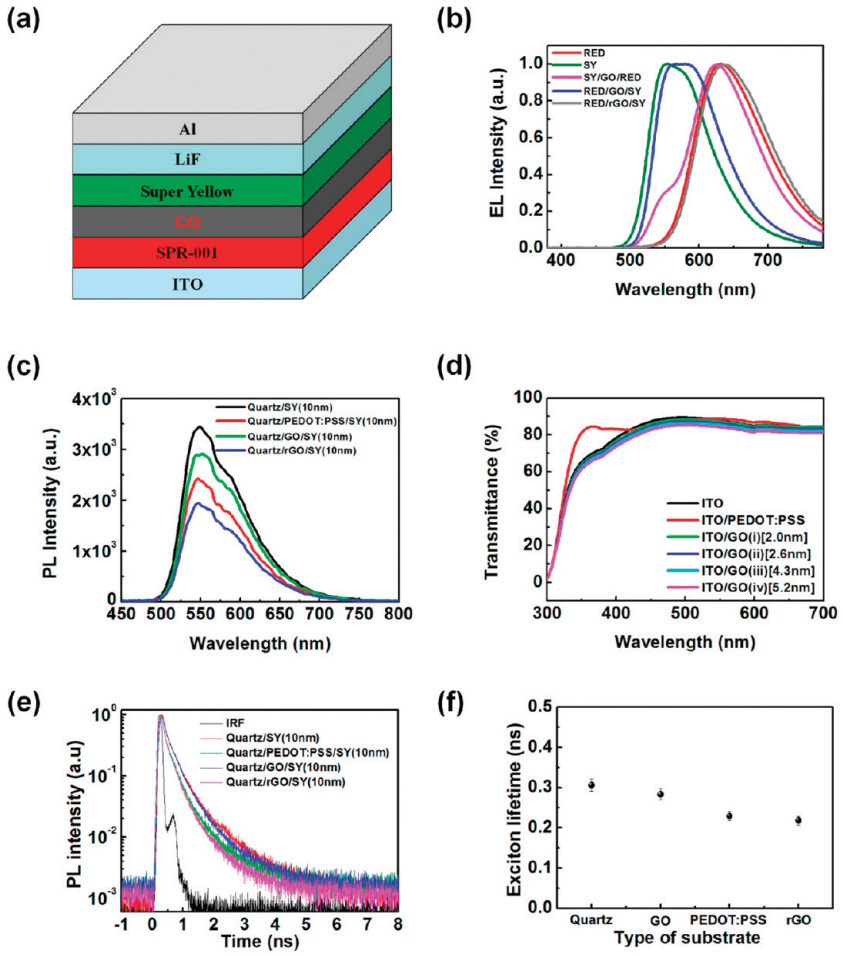

Figure 5. (a,b) Electron-blocking property of GO. Schematic energy diagrams of the devices used to evaluate the electron-blocking behavior of GO: (a) ITO/SPR-001/GO or rGO/super yellow/LiF/Al. (b) Electroluminescence (EL) spectra of diverse device configurations. (c) Photoluminescence (PL) spectra of SY films on quartz, PEDOT:PSS/quartz, rGO/quartz, and GO/quartz substrates. (d) Transmittance of HTL (PEDOT:PSS, GO) measured using a UV−vis spectrometer. (e) Time-resolved PL signal of SY, PEDOT:PSS/SY, rGO/SY, and GO/SY films, measured by time-correlated single photon counting (TCSPC). (f) Exciton lifetime of SY, PEDOT:PSS/SY, rGO/SY, and GO/SY films.

confirmed that the EL spectra of pristine and briefly UV/O_3-treated polymer films (SPR-001 or SY) were nearly identical.

When the GO film was introduced between the SY and the SPR-001 layers (ITO/SY/GO/SPR-001/LiF/Al configuration), red emission (pink link) was dominant, as shown in Figure 5b. In contrast, a device with the reversed order of ITO/SPR-001/GO/SY/LiF/Al exhibited green emission (blue line) dominantly. This result suggests that the GO film effectively blocked the electron transport from the SY layer into the SPR-001 layer in the ITO/SPR-001/GO/SY/LiF/Al structure. Therefore, recombinations between the injected holes and electrons mainly occurred within the SY layer. The EL spectrum almost overlapped with that of the SY single-emitting-layer device, demonstrating the effective electron-blocking capabilities by GO film, although there was a small effect of red emission by the red shift. However, when the rGO film was inserted between the SPR-001 and SY layers (ITO/SPR-001/GO/SY/LiF/Al configuration), red emission (gray line) was dominant, which was entirely different from the devices with the GO films due to the lack of an electron-blocking effect from the small band gap rGO film. We note that the GO film effectively blocks the electron transfer and optimizes hole−electron recombinations within the emissive layer, finally increasing the device efficiency in PLEDs.

Photoluminescence (PL) measurement experiments also support the high device efficiency gained when using GO film. Among the PL intensities of SY film (10 nm), PEDOT:PSS/SY(10 nm), rGO/SY (10 nm), and GO/SY (10 nm) on quartz substrates, the PL intensity of PEDOT:PSS showed the lower value, as represented by the significant exciton quenching that occurred at the PEDOT:PSS/SY interface. However, PL quenching of GO/SY film was less than that of PEDOT:PSS/SY film according to a comparison of the PL intensities, as shown in Figure 5c. Larger PL quenching also occurs at the rGO/SY (10 nm) interface due to interconnectivity of the localized sp^2 sites in the reduction process of GO.[59] The exciton lifetime of SY was also measured by

TABLE 2. Exciton Lifetime of SY, PEDOT:PSS/SY, rGO/SY, and GO/SY Films

sample	$\tau_1(f_1)$ (ns)	$\tau_2(f_2)$ (ns)	χ^2	τ_{avr} (ns)
quartz/SY(10 nm)	0.793(0.14)	0.224(0.86)	1.881	0.306
quartz/PEDOT:PSS/SY(10 nm)	0.646(0.12)	0.171(0.88)	1.740	0.229
quartz/GO/SY(10 nm)	0.670(0.16)	0.206(0.84)	1.668	0.283
quartz/rGO/SY(10 nm)	0.590(0.12)	0.168(0.88)	1.856	0.218

TABLE 3. PL Quantum Efficiency (PLQE) for SY Films in Several Sample Configurations Measured Inside an Integrating Sphere with an Excitation Wavelength of 450 nm

configuration	PLQE (%)
quartz/SY(10 nm)	68
quartz/PEDOT:PSS/SY(10 nm)	45
quartz/GO/SY(10 nm)	51
quartz/rGO/SY(10 nm)	33

using time-correlated single photon counting (TCSPC) to investigate the exciton quenching of SY on the different substrates. The quartz/SY was prepared for reference. As shown in Figure 5e,f, TCSPC results were consistent with the steady-state PL results in Figure 5c. The exciton lifetimes at 550 nm decreased dramatically from 0.306 ns in the SY film on quartz to 0.229 ns on PEDOT:PSS. On the other hand, the significant decrease in the exciton lifetime was not found by replacing PEDOT:PSS with a GO layer. The exciton lifetime of SY on the GO layer at 550 nm is 0.283 ns, which is about 92% of the exciton lifetime of SY on quartz. It indicates that exciton quenching at the interface of GO and SY is much less than that at the interface of PEDOT:PSS and SY, as shown in Figure 5e,f and Table 2. The increase in the exciton lifetime is related to the increase in the device lifetime.[16] PL quantum efficiency (PLQE), measured inside an integrating sphere with an excitation wavelength of 450 nm, also supports this result, as shown in Table 3. The optical transmission spectra of different thicknesses of GO layers deposited on ITO/glass substrates are shown in Figure 5d. Although the transmittance decreases slightly with the thickness, there was no significant change in the transparence of the anode substrates with the thin GO.

CONCLUSION

We demonstrated a straightforward means of enhancing device efficiency by introducing wide band gap GO HTLs between the ITO and the active polymer instead of PEDOT:PSS. PLEDs with a GO interlayer perform better than both those with PEDOT:PSS and rGO, showing maximum luminance of 39 000 Cd/m^2 and maximum efficiency levels as high as 19.1 Cd/A (at 6.8 V). The luminous efficiencies with GO are approximately 2.2-fold higher than that with PEDOT:PSS and 4-fold higher than that with rGO. Furthermore, we determined the cause of greatly improved efficiency with observations of the EL spectra in an effort to evaluate the electron-blocking behaviors of the GO layer in the ITO/SPR-001/GO or rGO/SY/LiF/Al configuration, with a comparison of the PL intensities of PEDOT:PSS/active polymer (10 nm) and GO/active polymer (10 nm) samples to investigate exciton quenching. The GO layer provides an excellent alternative to PEDOT:PSS in optoelectronic devices such as OPVs and PLEDs.

EXPERIMENTAL METHODS

Synthesis of GO. Graphite oxide was synthesized by the modified Hummers method and exfoliated to give a brown dispersion of graphene oxide under ultrasonication.[60,61] The resulting graphene oxide (GO) was negatively charged over a wide pH condition, as the GO sheet had chemical functional groups of carboxylic acids.

Synthesis of rGO. The GO solution (10.0 mL, 0.50 mg/mL) was mixed with 10.0 μL of hydrazine solution (35 wt % in water, Aldrich) and 70.0 μL of ammonia solution (30%, Samchun). After stirring for 10 min, the reaction mixture was heated to 95 °C for 1 h to afford the reduced graphene oxide (rGO) solution used in this study.

PLED and PSC Fabrication. Two devices (PLEDs and PSCs) were fabricated on patterned ITO-coated glass substrates, which had been cleaned by a sequential ultrasonic treatment in acetone and isopropyl alcohol (IPA) and were then dried under a N_2 stream.

A negatively charged graphene oxide (GO) solution (0.5 mg mL^{-1}) at pH 3.3 was dropped after an oxygen plasma treatment to introduce a hydrophilic surface onto the ITO substrates. The dropped GO was maintained for a waiting period of 2 min and was then spun at 3000 rpm for 30 s. The above procedures were repeated to achieve the desired full coverage of the GO sheets.

For the PLEDs, SY solution dissolved in chlorobenzene (0.7 wt %) was spin-cast at 2000 rpm for 45 s on top of a GO layer, after which it was annealed at 80 °C for 30 min to obtain a 150 nm thick SY layer on the PLEDs. Finally, a 1 nm thick LiF layer and a 70 nm thick Al layer were thermally evaporated on the SY layer to complete the fabrication of the device.

For the PSCs, a P3HT solution dissolved in chlorobenzene (1.0 wt %) was spin-cast at 700 rpm for 60 s on top of a GO layer and was then annealed at 150 °C for 10 min to obtain a 100 nm thick P3HT layer on the PSCs. A 70 nm thick Al layer was thermally evaporated on the P3HT layer to complete the fabrication of the device.

PLED Device Characterization. The current density and luminance *versus* the applied voltage characteristics were measured using a Keithley 2400 source measurement unit and a Konica Minolta spectroradiometer (CS-2000).

PSC Device Characterization. Measurements were carried out with solar cells inside a glovebox using a high-quality optical fiber to guide the light from the solar simulator, which was equipped with a Keithley 2635A source measurement unit. The *J*−*V* curves of the devices were measured under AM 1.5G illumination at 100 mW/cm^2.

Electron Blocking of PLEDs. The devices for this part of the experiment were prepared along with the fabrication of the PLEDs. In addition, a SPR-001 solution dissolved in chlorobenzene (1.4 wt %) was spin-cast at 2000 rpm for 45 s on ITO, after which the polymer surface underwent a perform brief UV/O_3 treatment for the deposit of the GO film.

Characterizations. The surface roughness and thickness of the GO/Si were measured by AFM (Veeco, USA). A UV−vis

spectrometer (Varian Cary 5000) was utilized to measure the optical transmittance levels of the ITO, ITO/PEDOT:PSS, and GO/ITO. The PL intensities of the SY(10 nm)/quartz, SY(10 nm)/PEDOT:PSS/quartz, and SY(10 nm)/GO/quartz were measured using photoluminescence spectroscopy (Edinburgh Instruments Ltd.).

Time-Correlated Single Photon Counting Characterization. For measuring exciton lifetimes, time-correlated single photon counting (TCSPC) was performed. The second harmonic (SHG = 420 nm) of a tunable Ti:sapphire laser (Mira900, Coherent) with ~150 fs pulse width and 76 MHz repetition rate was used as an excitation source. The PL emission was spectrally resolved by using some collection optics and a monochromator (SP-2150i, Acton). The TCSPC module (PicoHarp, PicoQuant) with a MCP-PMT (R3809U-59, Hamamatsu) was used for ultrafast detection. The total instrument response function (IRF) for PL decay was less than 150 ps, and the temporal time resolution was less than 10 ps. The deconvolution of actual fluorescence decay and IRF was performed by using a fitting software (FlouFit, PicoQuant) to deduce the time constant associated with each exponential decay.

Conflict of Interest: The authors declare no competing financial interest.

Acknowledgment. This work was supported by the Midcareer Researcher Program (2010-0027764) and the research Foundation of Korea (2010-0028791). H.S.S. thanks the support by the WCU (World Class University) program (R31-2008-000-20012-0) and the grant (Code No. 2011-0031630) from the Center for Advanced Soft Electronics under the Global Frontier Research Program through the National Research Foundation funded by MEST of Korea.

Supporting Information Available: EL spectra of PLEDs with various configurations using PEDOT:PSS, rGO, and GO with different thickness as hole transport layers. This material is available free of charge *via* the Internet at http://pubs.acs.org.

REFERENCES AND NOTES

1. Burroughes, J. H.; Bradley, D. D. C.; Brown, A. R.; Marks, R. N.; Mackay, K.; Friend, R. H.; Burns, P. L.; Holmes, A. B. Light-Emitting Diodes Based on Conjugated Polymers. *Nature* **1990**, *347*, 539–541.
2. Friend, R. H.; Gymer, R. W.; Holmes, A. B.; Burroughes, J. H.; Marks, R. N.; Taliani, C.; Bradley, D. D. C.; Dos Santos, D. A.; Bredas, J. L.; Logdlund, M.; *et al.* Electroluminescence in Conjugated Polymers. *Nature* **1999**, *397*, 121–128.
3. Kim, J. Y.; Lee, K.; Coates, N. E.; Moses, D.; Nguyen, T. Q.; Dante, M.; Heeger, A. J. Efficient Tandem Polymer Solar Cells Fabricated by All-Solution Processing. *Science* **2007**, *317*, 222–225.
4. De Arco, L. G.; Zhang, Y.; Schlenker, C. W.; Ryu, K.; Thompson, M. E.; Zhou, C. W. Continuous, Highly Flexible, and Transparent Graphene Films by Chemical Vapor Deposition for Organic Photovoltaics. *ACS Nano* **2010**, *4*, 2865–2873.
5. D'Andrade, B. W.; Forrest, S. R. White Organic Light-Emitting Devices for Solid-State Lighting. *Adv. Mater.* **2004**, *16*, 1585–1595.
6. Gustafsson, G.; Cao, Y.; Treacy, G. M.; Klavetter, F.; Colaneri, N.; Heeger, A. J. Flexible Light-Emitting Diodes Made from Soluble Conducting Polymers. *Nature* **1992**, *357*, 477–479.
7. Ou, E. C. W.; Hu, L. B.; Raymond, G. C. R.; Soo, O. K.; Pan, J. S.; Zheng, Z.; Park, Y.; Hecht, D.; Irvin, G.; Drzaic, P.; *et al.* Surface-Modified Nanotube Anodes for High Performance Organic Light-Emitting Diode. *ACS Nano* **2009**, *3*, 2258–2264.
8. Ma, H.; Yip, H. L.; Huang, F.; Jen, A. K. Y. Interface Engineering for Organic Electronics. *Adv. Funct. Mater.* **2010**, *20*, 1371–1388.
9. Steim, R.; Kogler, F. R.; Brabec, C. J. Interface Materials for Organic Solar Cells. *J. Mater. Chem.* **2010**, *20*, 2499–2512.
10. Koch, N. Organic Electronic Devices and Their Functional Interfaces. *ChemPhysChem* **2007**, *8*, 1438–1455.
11. Ho, P. K. H.; Kim, J. S.; Burroughes, J. H.; Becker, H.; Li, S. F. Y.; Brown, T. M.; Cacialli, F.; Friend, R. H. Molecular-Scale Interface Engineering for Polymer Light-Emitting Diodes. *Nature* **2000**, *404*, 481–484.
12. Xu, Q. F.; Ouyang, J. Y.; Yang, Y.; Ito, T.; Kido, J. Ultrahigh Efficiency Green Polymer Light-Emitting Diodes by Nanoscale Interface Modification. *Appl. Phys. Lett.* **2003**, *83*, 4695–4697.
13. Kim, J. S.; Ho, P. K. H.; Murphy, C. E.; Seeley, A.; Grizzi, I.; Burroughes, J. H.; Friend, R. H. Electrical Degradation of Triarylamine-Based Light-Emitting Polymer Diodes Monitored by Micro-Raman Spectroscopy. *Chem. Phys. Lett.* **2004**, *386*, 2–7.
14. Kim, Y. H.; Lee, S. H.; Noh, J.; Han, S. H. Performance and Stability of Electroluminescent Device with Self-Assembled Layers of Poly(3,4-ethylenedioxythiophene)-Poly(styrenesulfonate) and Polyelectrolytes. *Thin Solid Films* **2006**, *510*, 305–310.
15. Van de Lagemaat, J.; Barnes, T. M.; Rumbles, G.; Shaheen, S. E.; Coutts, T. J.; Weeks, C.; Levitsky, I.; Peltola, J.; Glatkowski, P. Organic Solar Cells with Carbon Nanotubes Replacing In_2O_3:Sn as the Transparent Electrode. *Appl. Phys. Lett.* **2006**, *88*, 233503.
16. Kim, J. S.; Friend, R. H.; Grizzi, I.; Burroughes, J. H. Spin-Cast Thin Semiconducting Polymer Interlayer for Improving Device Efficiency of Polymer Light-Emitting Diodes. *Appl. Phys. Lett.* **2005**, *87*, 023506.
17. Yan, H.; Lee, P.; Armstrong, N. R.; Graham, A.; Evmenenko, G. A.; Dutta, P.; Marks, T. J. High-Performance Hole-Transport Layers for Polymer Light-Emitting Diodes. Implementation of Organosiloxane Cross-Linking Chemistry in Polymeric Electroluminescent Devices. *J. Am. Chem. Soc.* **2005**, *127*, 3172–3183.
18. Yang, X. H.; Muller, D. C.; Neher, D.; Meerholz, K. Highly Efficient Polymeric Electrophosphorescent Diodes. *Adv. Mater.* **2006**, *18*, 948–954.
19. Niu, Y. H.; Liu, M. S.; Ka, J. W.; Bardeker, J.; Zin, M. T.; Schofield, R.; Chi, Y.; Jen, A. K. Y. Crosslinkable Hole-Transport Layer on Conducting Polymer for High-Efficiency White Polymer Light-Emitting Diodes. *Adv. Mater.* **2007**, *19*, 300–304.
20. Lim, Y.; Park, Y. S.; Kang, Y.; Jang, D. Y.; Kim, J. H.; Kim, J. J.; Sellinger, A.; Yoon, D. Y. Hole Injection/Transport Materials Derived from Heck and Sol−Gel Chemistry for Application in Solution-Processed Organic Electronic Devices. *J. Am. Chem. Soc.* **2011**, *133*, 1375–1382.
21. Han, T. H.; Choi, M. R.; Woo, S. H.; Min, S. Y.; Lee, C. L.; Lee, T. W. Molecularly Controlled Interfacial Layer Strategy toward Highly Efficient Simple-Structured Organic Light-Emitting Diodes. *Adv. Mater.* **2012**, DOI: 10.1002/adma.201104316.
22. Nakayama, Y.; Morii, K.; Suzuki, Y.; Machida, H.; Kera, S.; Ueno, N.; Kitagawa, H.; Noguchi, Y.; Ishii, H. Origins of Improved Hole-Injection Efficiency by the Deposition of MoO_3 on the Polymeric Semiconductor Poly(dioctylfluorene-*alt*-benzothiadiazole). *Adv. Funct. Mater.* **2009**, *19*, 3746–3752.
23. Kabra, D.; Lu, L. P.; Song, M. H.; Snaith, H. J.; Friend, R. H. Efficient Single-Layer Polymer Light-Emitting Diodes. *Adv. Mater.* **2010**, *22*, 3194–3198.
24. Park, J. S.; Lee, B. R.; Lee, J. M.; Kim, J. S.; Kim, S. O.; Song, M. H. Efficient Hybrid Organic−Inorganic Light Emitting Diodes with Self-Assembled Dipole Molecule Deposited Metal Oxides. *Appl. Phys. Lett.* **2010**, *96*, 243306.
25. Lee, B. R.; Choi, H.; Park, J. S.; Lee, H. J.; Kim, S. O.; Kim, J. Y.; Song, M. H. Surface Modification of Metal Oxide Using Ionic Liquid Molecules in Hybrid Organic−Inorganic Optoelectronic Devices. *J. Mater. Chem.* **2011**, *21*, 2051–2053.
26. Lee, T. W.; Hwang, J.; Min, S. Y. Highly Efficient Hybrid Inorganic−Organic Light-Emitting Diodes by using Air-Stable Metal Oxides and a Thick Emitting Layer. *ChemSusChem* **2010**, *3*, 1021–1023.
27. Bolink, H. J.; Coronado, E.; Orozco, J.; Sessolo, M. Efficient Polymer Light-Emitting Diode Using Air-Stable Metal Oxides as Electrodes. *Adv. Mater.* **2009**, *21*, 79–82.

28. Shrotriya, V.; Li, G.; Yao, Y.; Chu, C. W.; Yang, Y. Transition Metal Oxides as the Buffer Layer for Polymer Photovoltaic Cells. *Appl. Phys. Lett.* **2006**, *88*, 073508.
29. Hamwi, S.; Meyer, J.; Winkler, T.; Riedl, T.; Kowalsky, W. P-Type Doping Efficiency of MoO_3 in Organic Hole Transport Materials. *Appl. Phys. Lett.* **2009**, *94*, 253307.
30. Chu, T. Y.; Chen, J. F.; Chen, S. Y.; Chen, C. J.; Chen, C. H. Highly Efficient and Stable Inverted Bottom-Emission Organic Light Emitting Devices. *Appl. Phys. Lett.* **2006**, *89*, 053503.
31. Tao, C.; Ruan, S. P.; Xie, G. H.; Kong, X. Z.; Shen, L.; Meng, F. X.; Liu, C. X.; Zhang, X. D.; Dong, W.; Chen, W. Y. Role of Tungsten Oxide in Inverted Polymer Solar Cells. *Appl. Phys. Lett.* **2009**, *94*, 043311.
32. Chan, I. M.; Hsu, T. Y.; Hong, F. C. Enhanced Hole Injections in Organic Light-Emitting Devices by Depositing Nickel Oxide on Indium Tin Oxide Anode. *Appl. Phys. Lett.* **2002**, *81*, 1899–1901.
33. Irwin, M. D.; Buchholz, B.; Hains, A. W.; Chang, R. P. H; Marks, T. J. P-Type Semiconducting Nickel Oxide as an Efficiency-Enhancing Anode Interfacial Layer in Polymer Bulk-Heterojunction Solar Cells. *Proc. Natl. Acad. Sci. U.S.A.* **2008**, *105*, 2783–2787.
34. Chu, C. W.; Chen, C. W.; Li, S. H.; Wu, E. H. E.; Yang, Y. Integration of Organic Light-Emitting Diode and Organic Transistor *via* a Tandem Structure. *Appl. Phys. Lett.* **2005**, *86*, 253503.
35. Li, G.; Chu, C. W.; Shrotriya, V.; Huang, J.; Yang, Y. Efficient Inverted Polymer Solar Cells. *Appl. Phys. Lett.* **2006**, *88*, 253503.
36. Zhang, D. D.; Feng, J.; Chen, L.; Wang, H.; Liu, Y. F.; Jin, Y.; Bai, Y.; Zhong, Y. Q.; Sun, H. B. Role of Fe_3O_4 as a p-Dopant in Improving the Hole Injection and Transport of Organic Light-Emitting Devices. *IEEE J. Quantum Electron.* **2011**, *47*, 591–596.
37. Lee, W. H.; Park, J.; Sim, S. H.; Jo, S. B.; Kim, K. S.; Hong, B. H.; Cho, K. Transparent Flexible Organic Transistors Based on Monolayer Graphene Electrodes on Plastic. *Adv. Mater.* **2011**, *23*, 1752–1756.
38. Bi, H.; Huang, F. Q.; Liang, J.; Xie, X. M.; Jiang, M. H. Transparent Conductive Graphene Films Synthesized by Ambient Pressure Chemical Vapor Deposition Used as the Front Electrode of CdTe Solar Cells. *Adv. Mater.* **2011**, *23*, 3202–3206.
39. Wang, Y.; Tong, S. W.; Xu, X. F.; Ozyilmaz, B.; Loh, K. P. Interface Engineering of Layer-by-Layer Stacked Graphene Anodes for High-Performance Organic Solar Cells. *Adv. Mater.* **2011**, *23*, 1514–1518.
40. Matyba, P.; Yamaguchi, H.; Eda, G.; Chhowalla, M.; Edman, L.; Robinson, N. D. Graphene and Mobile Ions: The Key to All-Plastic, Solution-Processed Light-Emitting Devices. *ACS Nano* **2010**, *4*, 637–642.
41. Wang, X.; Zhi, L. J.; Mullen, K. Transparent, Conductive Graphene Electrodes for Dye-Sensitized Solar Cells. *Nano Lett.* **2008**, *8*, 323–327.
42. Lee, D. W.; Hong, T. K.; Kang, D.; Lee, J.; Heo, M.; Kim, J. Y.; Kim, B. S.; Shin, H. S. Highly Controllable Transparent and Conducting Thin Films Using Layer-by-Layer Assembly of Oppositely Charged Reduced Graphene Oxides. *J. Mater. Chem.* **2011**, *21*, 3438–3442.
43. Yin, Z. Y.; Sun, S. Y.; Salim, T.; Wu, S. X.; Huang, X. A.; He, Q. Y.; Lam, Y. M.; Zhang, H. Organic Photovoltaic Devices Using Highly Flexible Reduced Graphene Oxide Films as Transparent Electrodes. *ACS Nano* **2010**, *4*, 5263–5268.
44. Wu, J. B.; Agrawal, M.; Becerril, H. A.; Bao, Z. N.; Liu, Z. F.; Chen, Y. S.; Peumans, P. Organic Light-Emitting Diodes on Solution-Processed Graphene Transparent Electrodes. *ACS Nano* **2010**, *4*, 43–48.
45. Pang, S. P.; Tsao, H. N.; Feng, X. L.; Mullen, K. Patterned Graphene Electrodes from Solution-Processed Graphite Oxide Films for Organic Field-Effect Transistors. *Adv. Mater.* **2009**, *21*, 3488–3491.
46. Novoselov, K. S.; Geim, A. K.; Morozov, S. V.; Jiang, D.; Zhang, Y.; Dubonos, S. V.; Grigorieva, I. V.; Firsov, A. A. Electric Field Effect in Atomically Thin Carbon Films. *Science* **2004**, *306*, 666–669.
47. Balandin, A. A.; Ghosh, S.; Bao, W. Z.; Calizo, I.; Teweldebrhan, D.; Miao, F.; Lau, C. N. Superior Thermal Conductivity of Single-Layer Graphene. *Nano Lett.* **2008**, *8*, 902–907.
48. Zhu, Y. W.; Murali, S.; Cai, W. W.; Li, X. S.; Suk, J. W.; Potts, J. R.; Ruoff, R. S. Graphene and Graphene Oxide: Synthesis, Properties, and Applications. *Adv. Mater.* **2010**, *22*, 3906–3924.
49. Chen, H.; Muller, M. B.; Gilmore, K. J.; Wallace, G. G.; Li, D. Mechanically Strong, Electrically Conductive, and Biocompatible Graphene Paper. *Adv. Mater.* **2008**, *20*, 3557–3561.
50. Loh, K. P.; Bao, Q. L.; Eda, G.; Chhowalla, M. Graphene Oxide as a Chemically Tunable Platform for Optical Applications. *Nat. Chem.* **2010**, *2*, 1015–1024.
51. Li, X. L.; Wang, X. R.; Zhang, L.; Lee, S. W.; Dai, H. J. Chemically Derived, Ultrasmooth Graphene Nanoribbon Semiconductors. *Science* **2008**, *319*, 1229–1232.
52. Eda, G.; Fanchini, G.; Chhowalla, M. Large-Area Ultrathin Films of Reduced Graphene Oxide as a Transparent and Flexible Electronic Material. *Nat. Nanotechnol.* **2008**, *3*, 270–274.
53. Eda, G.; Chhowalla, M. Chemically Derived Graphene Oxide: Towards Large-Area Thin-Film Electronics and Optoelectronics. *Adv. Mater.* **2010**, *22*, 2392–2415.
54. Li, S. S.; Tu, K. H.; Lin, C. C.; Chen, C. W.; Chhowalla, M. Solution-Processable Graphene Oxide as an Efficient Hole Transport Layer in Polymer Solar Cells. *ACS Nano* **2010**, *4*, 3169–3174.
55. Yun, J.; Yeo, J.; Kim, J.; Jeong, H.; Kim, D.; Noh, Y.; Kim, S.; Ku, B.; Na, S. Solution-Processable Reduced Graphene Oxide as a Novel Alternative to PEDOT:PSS Hole Transport Layers for Highly Efficient and Stable Polymer Solar Cells. *Adv. Mater.* **2011**, *23*, 4923–4928.
56. Zhong, Z.; Dai, Y. F.; Ma, D. G.; Wang, Z. Y. Facile Synthesis of Organo-Soluble Surface-Grafted All-Single-Layer Graphene Oxide as Hole-Injecting Buffer Material in Organic Light-Emitting Diodes. *J. Mater. Chem.* **2011**, *21*, 6040–6045.
57. Yang, J.; Heo, M.; Lee, H. J.; Park, S. M.; Kim, J. Y.; Shin, H. S. Reduced Graphene Oxide (rGO)-Wrapped Fullerene (C_{60}) Wires. *ACS Nano* **2011**, *5*, 8365–8371.
58. Gunes, S.; Neugebauer, H.; Sariciftci, N. S. Conjugated Polymer-Based Organic Solar Cells. *Chem. Rev.* **2007**, *107*, 1324–1338.
59. Eda, G.; Lin, Y. Y.; Mattevi, C.; Yamaguchi, H.; Chen, H. A.; Chen, I. S.; Chen, C. W.; Chhowalla, M. Blue Photoluminescence from Chemically Derived Graphene Oxide. *Adv. Mater.* **2010**, *22*, 505–509.
60. Hummers, W. S.; Offeman, R. E. Preparation of Graphitic Oxide. *J. Am. Chem. Soc.* **1958**, *80*, 1339–1339.
61. Li, D.; Muller, M. B.; Gilje, S.; Kaner, R. B.; Wallace, G. G. Processable Aqueous Dispersions of Graphene Nanosheets. *Nat. Nanotechnol.* **2008**, *3*, 101–105.